

©2004 IEEE. Personal use of this material is permitted. However, permission to reprint/republish this material for advertising or promotional purposes or for creating new collective works for resale or redistribution to servers or lists, or to reuse any copyrighted component of this work in other works must be obtained from the IEEE.

Copyright and all rights therein are retained by authors or by other copyright holders. All persons copying this information are expected to adhere to the terms and constraints invoked by each author's copyright. In most cases, these works may not be reposted without the explicit permission of the copyright holder.

This copyright notice is taken from the IEEE PSPB Operations Manual, section 8.1.10 entitled "Electronic Information Dissemination". At the time of this notice, this section is posted at

[http://www.ieee.org/portal/index.jsp?pageID=corp\\_level1&path=about/documentation/copyright&file=policies.xml&xsl=generic.xsl](http://www.ieee.org/portal/index.jsp?pageID=corp_level1&path=about/documentation/copyright&file=policies.xml&xsl=generic.xsl)

# Neural-Network Approaches to Electromagnetic-Based Modeling of Passive Components and Their Applications to High-Frequency and High-Speed Nonlinear Circuit Optimization

Xiaolei Ding, *Student Member, IEEE*, Vijay K. Devabhaktuni, *Student Member, IEEE*, Biswarup Chattaraj, Mustapha C. E. Yagoub, *Member, IEEE*, Makarand Deo, *Student Member, IEEE*, Jianjun Xu, *Student Member, IEEE*, and Qi Jun Zhang, *Senior Member, IEEE*

**Abstract**—In this paper, artificial neural-network approaches to electromagnetic (EM)-based modeling in both frequency and time domains and their applications to nonlinear circuit optimization are presented. Through accurate and fast EM-based neural models of passive components, we enable consideration of EM effects in high-frequency and high-speed computer-aided design, including component's geometrical/physical parameters as optimization variables. Formulations for standard frequency-domain neural modeling approach, and recent time-domain neural modeling approach based on state-space concept, are described. A new EM-based time-domain neural modeling approach combining existing knowledge in the form of equivalent circuits (ECs), with state-space equations (SSEs) and neural networks (NNs), called the EC-SSE-NN, is proposed. The EC-SSE-NN models allow EM behaviors of passive components in the circuit to interact with nonlinear behaviors of active devices, and facilitate nonlinear circuit optimization in the time domain. An automatic mechanism for EM data generation, which can lead to efficient training of neural models for EM components, is presented. Demonstration examples including EM-based frequency-domain optimization of a three-stage amplifier, time-domain circuit optimization in a multilayer printed circuit board, including geometrical/physical-oriented neural models of power-plane effects, and EM-based optimization of a high-speed interconnect circuit with embedded passive terminations and nonlinear buffers in the time domain are presented.

**Index Terms**—Electromagnetic (EM), embedded passives, modeling, neural networks, optimization, simulation.

Manuscript received January 21, 2003; revised May 26, 2003. This work was supported in part by the Natural Sciences and Engineering Research Council of Canada, by Micronet, a Canadian Network of Centres of Excellence on Microelectronic Devices, Circuits, and Systems, and by Nortel Networks. The work on neural modeling of embedded passives was supported by the National Center for Manufacturing Sciences/Advanced Embedded Passives Technology Consortium under the U.S. Department of Commerce, National Institute of Standards and Technology, and Advanced Technology Program Cooperative Agreement 70NANB8H4025.

X. Ding, V. K. Devabhaktuni, M. Deo, J. Xu, and Q. J. Zhang are with the Department of Electronics, Carleton University, Ottawa, ON, Canada K1S 5B6.

B. Chattaraj was with the Department of Electronics, Carleton University, Ottawa, ON, Canada K1S 5B6. He is now with the Electrical and Computer Engineering Department, University of Illinois, Chicago, IL 60612 USA.

M. C. E. Yagoub is with the School of Information Technology Engineering, University of Ottawa, Ottawa, ON, Canada K1N 6N5.

Digital Object Identifier 10.1109/TMTT.2003.820889

## I. INTRODUCTION

ELECTROMAGNETIC (EM)-BASED modeling and optimization are important toward first-pass success of high-frequency and high-speed electronic circuit design [1], [2]. In recent years, an EM-oriented computer-aided design (CAD) approach based on artificial neural networks (ANNs) has gained recognition [3], [4]. Accurate and fast neural models can be developed from measured or simulated EM data. These neural models can be used in place of CPU-intensive detailed EM models to significantly speed up electronic circuit design, while maintaining EM-level accuracies. ANNs have been applied to modeling and design of a variety of components and circuits such as bends [5], embedded passive components [6], transmission-line components [7], [8], field-effect transistors (FETs) [9], vias [10], coplanar waveguide (CPW) components [11], spiral inductors [12], amplifiers [13], and filters [4].

Several EM-ANN-based CAD methods have been proposed in the RF/microwave CAD community. In [11], multilayer perceptrons (MLPs) neural networks were trained to learn EM behaviors of CPW components such as bends and junctions from frequency-domain EM simulations. Following this, accurate and fast EM-based design and optimization of CPW circuits was demonstrated using these neural models. A recent trend in the microwave-ANN area is knowledge-based approaches to efficient EM-based modeling and design, which advocates the use of existing knowledge such as conventional empirical models together with neural networks. Pioneering works in this direction include knowledge-based neural networks [9], difference network [10], prior knowledge input network [14], and space-mapped neural networks [5]. Neural model development using these knowledge approaches needs fewer EM simulations (or training data) and shorter training time, thereby facilitating cost-effective neural-based high-frequency circuit design and optimization.

The need for large-signal analysis of microwave circuits consisting of both active devices and passive components demands powerful nonlinear CAD methodologies [1], [15]. In this paper, we present EM-based neural modeling of passive components

and their applications to high-frequency and high-speed nonlinear circuit optimization in both frequency and time domains, including component's geometrical/physical parameters as optimization variables. The first step in this direction is to realize EM-based neural models in both frequency- and time-domain formats, compatible with the framework of existing CAD tools. Standard frequency-domain neural modeling approach involving training of neural networks from frequency-domain EM training data, which consists of  $S$ -parameters versus geometrical/physical parameters and frequency, is summarized.

Development of EM-based time-domain neural network models is a new research topic. A recent state-space equation-neural network (SSE-NN) approach [16] based on the state-space concept that facilitates development of time-domain neural models from frequency-domain EM data is described. Motivated by the knowledge-based approaches, we further propose an equivalent circuit-state-space equation-neural network (EC-SSE-NN) method for time-domain neural modeling that combines existing knowledge in the form of equivalent circuits (ECs) and empirical formulas with the SSE-NN. The EC-SSE-NN method aims to achieve a time-domain model with fewer expensive EM training data without sacrificing model accuracy. Incorporation of frequency- and time-domain neural models including the proposed EC-SSE-NN models into the nonlinear circuit equations for enabling EM-based nonlinear circuit optimization is formulated. The neural models allow EM behaviors of passive components in the circuit to interact with nonlinear behaviors of active devices. To further strengthen various approaches to EM-based neural modeling, an automatic mechanism for EM data generation is also presented.

In Sections II and III, formulations for standard frequency-domain neural modeling and recent time-domain neural modeling are presented. The proposed EC-SSE-NN approach for efficient time-domain neural model development from frequency-domain neural network training and the proposed automatic mechanism for EM data generation are presented in Section IV. In Section V, systematic methods for incorporating frequency- and time-domain neural models into harmonic balance (HB) and time-domain nonlinear circuit equations respectively, are derived. Section VI presents examples of EM-based optimization of a three-stage amplifier circuit in the frequency domain, time-domain circuit optimization in a multilayer printed circuit board (PCB) including geometrical/physical-oriented neural models of power-plane effects, and EM-based signal integrity analysis and optimization of a high-speed very large scale integration (VLSI) interconnect circuit with embedded passive terminations and nonlinear buffers. Finally, Section VII presents conclusions.

## II. FREQUENCY-DOMAIN NEURAL MODEL

Frequency-domain neural models are important for CAD such as nonlinear optimization of amplifier circuits in the frequency domain. A frequency-domain neural model represents  $S$ -parameters of a passive component with the speed of empirical models, but with accuracy comparable to detailed EM models [3], [9]. In this section, formulation for training

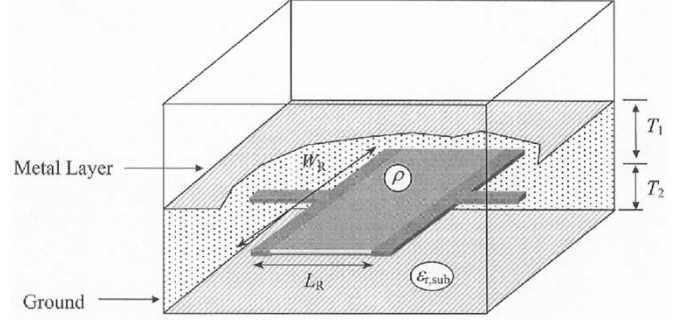


Fig. 1. Geometrical structure of embedded resistor in multilayer PCBs. Various ANN approaches including the proposed EC-SSE-NN are used to develop neural models of the resistor from EM data.

frequency-domain neural models from frequency-domain EM data is presented. Let  $\mathbf{x}$  represent an  $N_x$ -vector containing the external inputs (stimuli) and  $\mathbf{y}$  represent an  $N_y$ -vector containing the outputs (responses) of a passive component. For example,  $\mathbf{x}$  could contain geometrical parameters such as length ( $L_R$ ) and width ( $W_R$ ) of an embedded resistor, shown in Fig. 1, and signal frequency  $\omega$  and  $\mathbf{y}$  could contain corresponding  $Y$ - or  $S$ -parameters. Let  $\mathbf{f}$  represent a detailed EM relationship between  $\mathbf{x}$  and  $\mathbf{y}$ , i.e.,

$$\mathbf{y} = \mathbf{f}(\mathbf{x}) \quad (1)$$

to be modeled by a neural network. Information of  $\mathbf{f}$  can be typically accessed through detailed EM simulation software

$$\mathbf{d} = \mathbf{g}(\mathbf{x}) \quad (2)$$

also referred to as an EM simulator. We introduce a terminology for simulator “ $\mathbf{g}$ ” and refer to it as a “*data generator*.” For a given input  $\mathbf{x}$ , data generator  $\mathbf{g}(\mathbf{x})$  can be used to compute the outputs  $\mathbf{d}$ . Data generation involves repetitive use of  $\mathbf{g}$  to obtain sample pairs  $(\mathbf{x}_k, \mathbf{d}_k)$ , where  $k$  is the sample index. These sample pairs are divided into training and test sets. We define  $T_r$  and  $T_e$  as index sets of training and test data, respectively. The purpose of neural-network modeling is to develop a fast neural model

$$\tilde{\mathbf{y}} = \mathbf{f}_{\text{ANN}}(\mathbf{x}, \mathbf{w}) \quad (3)$$

that accurately represents  $\mathbf{g}$ . Here,  $\mathbf{f}_{\text{ANN}}$  is a neural network trained to learn  $\mathbf{g}$  from training data  $(\mathbf{x}_k, \mathbf{d}_k)$ ,  $k \in T_r$ ,  $\tilde{\mathbf{y}}$  is an  $N_y$ -vector of neural model responses, and  $\mathbf{w}$  is an ANN weight vector [3].

The MLP network [4] is the most commonly used neural network. For the purpose of ANN training, an error function  $E(\mathbf{w})$  is defined as

$$E(\mathbf{w}) = \frac{1}{2} \sum_{k \in T_r} \sum_{j=1}^{N_y} (\tilde{y}_{jk} - d_{jk})^2. \quad (4)$$

Here,  $\tilde{y}_{jk}$  is the  $j$ th element of the neural-network output  $\tilde{\mathbf{y}}(\mathbf{x}_k)$ , and  $d_{jk}$  is the  $j$ th element of corresponding data output  $\mathbf{d}_k$ . The objective of neural-network training is to adjust  $\mathbf{w}$  such that  $E(\mathbf{w})$  is minimized. Following (4), we can also define a

test error and use test data  $(\mathbf{x}_k, \mathbf{d}_k)$  and  $k \in T_e$  to independently assess the quality of the trained neural model. The trained neural model  $\mathbf{f}_{\text{ANN}}$  can be used in place of a CPU-intensive EM simulator to provide fast EM information needed during frequency-domain simulation and optimization.

### III. TIME-DOMAIN NEURAL MODEL

Time-domain models are important for transient analysis and design of nonlinear circuits such as minimization of signal delay and crosstalk in high-speed VLSI interconnect networks [17], [18] and ground noise minimization in integrated-circuit (IC) packages [19]. Conventional time-domain models such as equivalent-circuit-based models and quasi-static semianalytical models are not sufficient for CAD of high-speed circuits. As such, there is a need for time-domain models that include detailed EM effects. Time-domain neural modeling for passive components is a relatively new subject. In this section, our recent SSE-NN approach [16] for training time-domain neural models from frequency-domain EM data is presented.

In the time-domain formulation, we define that neural model inputs  $\mathbf{x}$  contains geometrical and physical parameters only (signal frequency  $\omega$  is not included). The bottleneck in the SSE-NN approach is to establish a link between component's geometrical parameters and time-domain responses through a neural-network model. We begin with transfer functions (TFs), also called polynomial rational functions, to represent admittances of a two-port passive component as [16]

$$H_{ij} = Y_{ij}(s) = \frac{b_{ij}^{(0)} + b_{ij}^{(1)}s + \dots + b_{ij}^{(n-1)}s^{n-1} + b_{ij}^{(n)}s^n}{a^{(0)} + a^{(1)}s + \dots + a^{(n-1)}s^{n-1} + s^n}, \quad (5)$$

$j = 1, 2; \quad i = j, \dots, 2.$

Here,  $s = j\omega$ , and  $n$  represents effective order of high-frequency behaviors of the passive component. As an example, using the definition  $Y_{11}(s) = I_1(s)/V_1(s)$  together with the inverse Laplace transform, time-domain voltage  $v_1(t)$  and current  $i_1(t)$  are related via coefficients  $a$ 's and  $b$ 's. The next challenge is to relate these TF coefficients to geometrical/physical parameters  $\mathbf{x}$ .

Let  $\mathbf{p}_{\text{TF}}$  be a real  $N_{\text{TF}}$ -vector of TF coefficients given by (6), shown at the bottom of this page.

For a given  $\mathbf{p}_{\text{TF}}$ , i.e., a fixed set of real values of the coefficients, (5) represents admittances of the passive component (as pure functions of frequency) for one geometry. In order to develop an EM-based neural model that represents the continuous relationship between geometrical parameters (i.e.,  $\mathbf{x}$ ) of the passive component and its  $Y$ -/S-parameters, we train an MLP neural network  $\mathbf{h}_{\text{ANN}}$  such that

$$\tilde{\mathbf{p}}_{\text{TF}} = \mathbf{h}_{\text{ANN}}(\mathbf{x}, \mathbf{w}_{\text{TF}}) \quad (7)$$

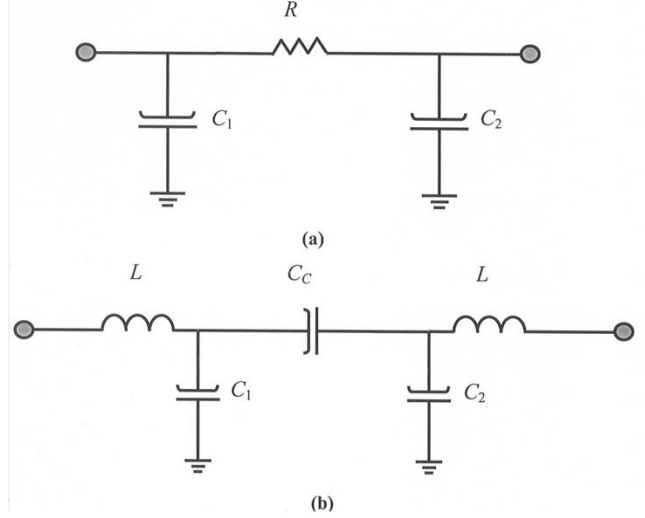


Fig. 2. Lumped ECs of: (a) embedded resistor and (b) embedded capacitor to be used as EC sub-models in the EC-SSE-NN approach.

where  $\mathbf{w}_{\text{TF}}$  is a vector of neural-network internal weights in  $\mathbf{h}_{\text{ANN}}$ . Following this, we utilize the SSEs to express the time-domain responses as

$$\begin{cases} \dot{\mathbf{v}}(t) = \mathbf{A}\mathbf{v}(t) + \mathbf{B}\mathbf{u}(t) \\ \mathbf{i}(t) = \mathbf{C}\mathbf{v}(t) + \mathbf{D}\mathbf{u}(t) \end{cases} \quad (8)$$

where matrices  $\mathbf{A}$ ,  $\mathbf{B}$ ,  $\mathbf{C}$ , and  $\mathbf{D}$  are formulated using the coefficients  $\tilde{\mathbf{p}}_{\text{TF}}$  estimated by  $\mathbf{h}_{\text{ANN}}$ [16]. In (8),  $\mathbf{v}(t)$  represents state variables, and  $\mathbf{u}(t)$  and  $\mathbf{i}(t)$  are input voltage and output current waveforms respectively. In summary, (7) and (8) form an EM-based time-domain SSE-NN model of the passive component under consideration.

### IV. EC-SSE-NN TIME-DOMAIN MODELING APPROACH

In this section, we extend the SSE-NN approach into an EC-SSE-NN technique that further strengthens EM-based time-domain neural modeling from frequency-domain EM data by exploiting available knowledge in the form of lumped ECs and empirical equations of the passive components. The proposed EC-SSE-NN can result in time-domain neural models with enhanced accuracies as compared to the SSE-NN, when the same amounts of EM data are used.

#### A. Existing Knowledge: ECs

A rich variety of ECs that approximate high-frequency behaviors of electrical components are available, e.g., ECs for embedded passives, shown in Fig. 2. Let values of all lumped elements in the EC of a given passive component be represented by a real  $N_{\text{EC}}$ -vector  $\mathbf{p}_{\text{EC}}$ . An EC model typically provides an approximation of the component behavior, but the accuracy may not be as good as that of EM. Our proposed EC-SSE-NN approach exploits the fundamental information provided by an

$$\mathbf{p}_{\text{TF}} = \left[ a^{(0)}, a^{(1)}, \dots, a^{(n-1)}, \quad b_{11}^{(0)}, b_{11}^{(1)}, \dots, b_{11}^{(n)}, b_{21}^{(0)}, b_{21}^{(1)}, \dots, b_{21}^{(n)}, b_{22}^{(0)}, b_{22}^{(1)}, \dots, b_{22}^{(n)} \right]^T \quad (6)$$

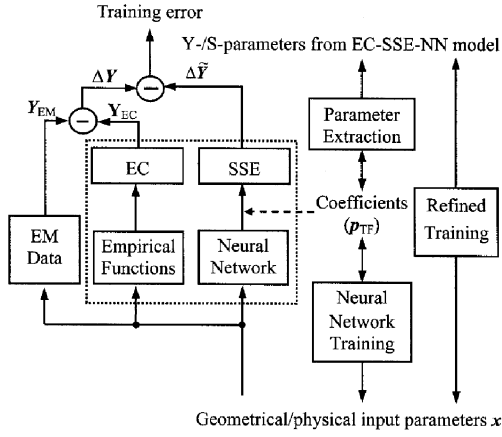


Fig. 3. Structure of the proposed EC–SSE–NN model showing the inputs, EC, SSE–NN sub-models, and the outputs.

EC and makes up for missing EM information by an additional neural-based sub-model.

### B. EC–SSE–NN Model Structure

We propose to combine the EC sub-model with an SSE–NN sub-model to form a new model, namely, the EC–SSE–NN model in a structural format, as illustrated in Fig. 3. Inputs  $\mathbf{x}$  to EC–SSE–NN model consist of geometrical/physical parameters of a passive component and outputs are EM-based time-domain responses. For a given  $\mathbf{x}$ , let  $Y$ -parameters of EM data and the EC sub-model be denoted as  $\mathbf{Y}_{EM}$  and  $\mathbf{Y}_{EC}$ , respectively. The difference  $\Delta\mathbf{Y}$  between  $\mathbf{Y}_{EM}$  and  $\mathbf{Y}_{EC}$  is to be utilized in a manner similar to the frequency-domain neural modeling approach of [10]. The difference in parameter  $Y_{ij}$  can be expressed as

$$\Delta Y_{ij}(s_l) = Y_{ij,EM}(s_l) - Y_{ij,EC}(s_l), \quad j = 1, 2; \quad i = j, \dots, 2 \quad (9)$$

at a given frequency  $s_l = j\omega_l$ , where  $l$  is the frequency index. An MLP neural network  $\mathbf{h}_{ANN}$  in the SSE–NN sub-model maps geometrical/physical parameters  $\mathbf{x}$  of passive component to  $Y$ -parameters by extracting TF coefficients  $\mathbf{p}_{TF}$  by learning frequency-domain difference  $(\mathbf{x}, \Delta\mathbf{Y})$ . The SSEs in the SSE–NN sub-model are used to provide time-domain responses corresponding to  $\Delta\tilde{\mathbf{Y}}$ . At the higher level of the EC–SSE–NN model, summation of time-domain responses from an EC and SSE–NN yields overall time-domain responses including EM effects for any given geometrical/physical inputs  $\mathbf{x}$ .

### C. EC–SSE–NN Model Training

A systematic training of EC–SSE–NN models is presented in this section. We begin with a given (or best available) EC of the passive component, and EM data  $(\mathbf{x}_k, \mathbf{d}_k)$ , where  $k$  is the index of data samples. Typically, inputs  $\mathbf{x}$  include geometrical dimensions and material parameters. In other words, unlike in the frequency domain, when we refer to  $\mathbf{x}$  here, it excludes frequency. The outputs  $\mathbf{d}$  generated from detailed EM simulations are the two-port  $S$ -parameters. For ease of implementation, we use  $Y$ - and  $S$ -parameters interchangeably in various phases of model development and in model usage.  $Y$ -parameter format is

used when dealing with difference data and when combining the EC and SSE–NN in order to provide a time-domain model consistent with Kirchhoff’s laws. An  $S$ -parameter format is used to test and refine the overall EC–SSE–NN accuracy with respect to original EM data.

The first phase (parameter extraction (PE) or PE phase) of training is a process to be repeated for every  $k$ th geometry,  $k \in T_r$ . The  $S$ -parameter EM training data are converted into equivalent  $Y$ -parameters and the admittance mismatch  $\Delta\mathbf{Y}$  between  $\mathbf{Y}_{EM}$  and  $\mathbf{Y}_{EC}$  is evaluated. This leads to sample pairs  $(\mathbf{x}_k, \Delta\mathbf{Y}(s_l))$ , where  $l$  is the frequency index. A PE is carried out for the  $k$ th geometrical configuration of the passive component to obtain corresponding TF coefficients  $\mathbf{p}_{TF}$ . We define a new error function  $E(\mathbf{p}_{TF,k})$  for the  $k$ th geometry as

$$E(\mathbf{p}_{TF,k}) = \frac{1}{2} \sum_{j=1}^2 \sum_{i=j}^2 \sum_{l=1}^{N_s} |H_{ij}(\mathbf{p}_{TF,k}, s_l) - \Delta Y_{ij}(s_l)|^2 \quad (10)$$

where  $H_{ij}$  is defined in (5), and  $N_s$  is the number of frequencies at which EM data has been generated. The objective of the  $k$ th PE is to determine  $\mathbf{p}_{TF,k}$  that minimizes  $E(\mathbf{p}_{TF,k})$ . As mentioned earlier, PE is repeated for all  $k \in T_r$ , i.e., for all geometrical configurations in the training data. At the end of this phase, sample pairs  $(\mathbf{x}_k, \mathbf{p}_{TF,k})$  are available. The PE process for each geometry is a nonlinear optimization in  $\mathbf{p}_{TF}$ -space constrained by passivity conditions derived following [20].

In the second phase (training phase), a three-layer MLP network  $\mathbf{h}_{ANN}$  with  $N_x$  inputs and  $N_{TF}$  outputs is trained to learn sample pairs  $(\mathbf{x}_k, \mathbf{p}_{TF,k})$  for all  $k, k \in T_r$ . For training purpose, we define an error function  $E_1(\mathbf{w}_{TF})$  as

$$E_1(\mathbf{w}_{TF}) = \frac{1}{2} \sum_{k \in T_r} \|(\mathbf{h}_{ANN}(\mathbf{x}_k, \mathbf{w}_{TF}) - \mathbf{p}_{TF,k})\|^2. \quad (11)$$

The objective of neural-network training is to adjust  $\mathbf{w}_{TF}$  such that  $E_1(\mathbf{w}_{TF})$  is minimized. At the end of this phase, a neural model that accurately represents the nonlinear relationship between  $\mathbf{x}$  and  $\mathbf{p}_{TF}$  is available. In the third phase (model refinement phase), the  $Y$ -parameters from the SSE–NN sub-model (which is a difference) are added to  $Y$ -parameter approximations from the EC sub-model to produce overall EC–SSE–NN  $Y$ -parameters, which are then converted into equivalent  $S$ -parameters. Following this, the EM training data is used to further refine the EC–SSE–NN model in terms of accuracy. Let  $\mathbf{S}_{EC-SSE-NN}$  represent  $S$ -parameters from the overall EC–SSE–NN model as a function of neural-network weights  $\mathbf{w}_{TF}$  and frequency. The objective here is to adjust  $\mathbf{w}_{TF}$  such that the error function

$$E_2(\mathbf{w}_{TF}) = \frac{1}{2} \sum_{k \in T_r} \sum_{j=1}^2 \sum_{i=j}^2 \sum_{l=1}^{N_s} |S_{ij,EM}(\mathbf{x}_k, s_l) - S_{ij,EC-SSE-NN}(\mathbf{x}_k, \mathbf{w}_{TF}, s_l)|^2 \quad (12)$$

is minimized. In (12),  $\mathbf{S}_{EM}$  represents  $S$ -parameters from EM data as functions of geometry  $\mathbf{x}_k$  and frequency  $s_l$ . At the end of this step, a refined EC–SSE–NN model is available for independent quality assessment and usage.

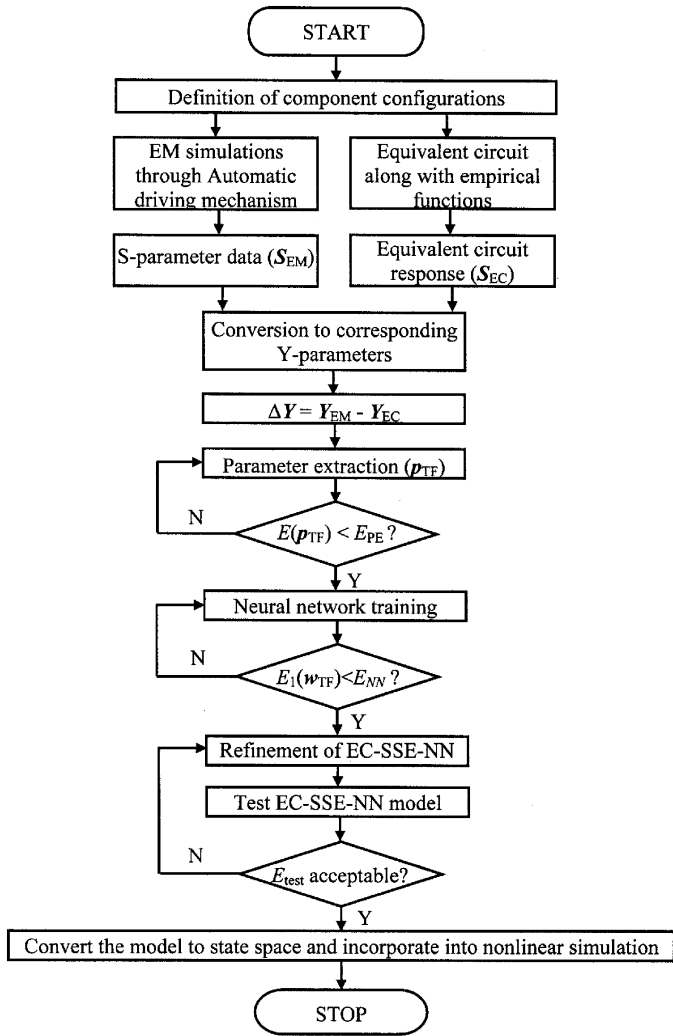


Fig. 4. Flowchart showing systematic development of an EC-SSE-NN model through various phases.  $E_{PE}$  and  $E_{NN}$  are user-specified accuracy criteria for PE and neural-network training, respectively, and  $E_{test}$  is the average test error of the EC-SSE-NN model.

In the final phase (testing phase), an independent set of frequency-domain EM data never seen during training is used to test the quality of the EC-SSE-NN model. If the test error is acceptable, the model is ready to be used for CAD. Otherwise, model refinement is continued using incremental EM data. A flowchart demonstrating the EC-SSE-NN model development process is shown in Fig. 4. The presence of SSEs in our EC-SSE-NN approach enables incorporation of trained models into nonlinear circuit equations to be used in time-domain EM-based circuit optimization.

#### D. Automation Mechanism for EM Data Generation

In general, training of EM-based neural models including the proposed EC-SSE-NN require EM data, e.g.,  $S$ -parameters versus geometrical/physical parameters of a passive component. This necessitates repetitive EM simulation for different values of geometrical/physical parameters. The conventional manual operation of EM simulator for this purpose is cumbersome and demands constant human involvement. To overcome this challenge, we formulated an automatic mechanism for

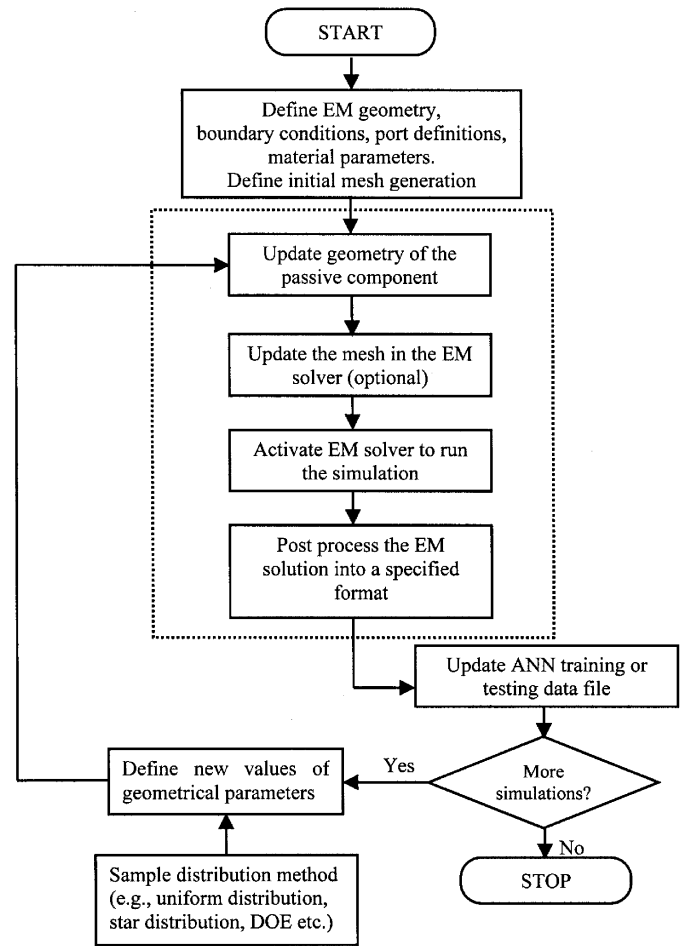


Fig. 5. Flowchart summarizing various steps involved in the proposed automatic mechanism for efficient EM data generation. The mechanism has been used to develop planar-EM and 3-D-EM drivers. Sample distributions such as uniform distribution and star distribution [3], [4] are used to guide the selection of new samples.

EM data generation, as shown in Fig. 5, which is implemented into a computer-based process. Several steps involved in the EM data generation are integrated into a unified mechanism. The EM setup is defined only once before beginning the data generation. Whenever the geometry changes, the driving mechanism automatically updates inputs to the EM solver, activates EM simulation, and processes EM solution into a form suitable for ANN training. The proposed approach makes data generation convenient, reduces human workload, and avoids risk of human-induced data errors. Several drivers for driving EM data generation such as a planar-EM driver and three-dimensional (3-D)-EM driver have been developed, and they helped to expedite the demonstration examples.

## V. INCORPORATION OF EM-BASED NEURAL MODELS INTO NONLINEAR CIRCUIT SIMULATION

### A. HB-Based Nonlinear Simulation

The HB method is an important technique for large-signal simulation of nonlinear periodic circuits [21], [22]. In the HB method, the circuit under consideration is divided into linear and nonlinear subnetworks. At high frequency, the EM effect of passive part of the circuit needs to be represented. An EM-based

neural model of a passive component can be included as an additional linear subnetwork. The overall HB equation can then be written as

$$\mathbf{I}(\mathbf{V}) + j\boldsymbol{\Omega}\mathbf{Q}(\mathbf{V}) + \mathbf{Y}\mathbf{V} + \mathbf{Y}_{\text{ANN,EM}}\mathbf{V} + \mathbf{I}_{ss} = 0 \quad (13)$$

where  $\mathbf{Y}$  is the nodal admittance matrix of linear subnetwork,  $\mathbf{V}$  represents voltages in the circuit,  $\mathbf{I}(\mathbf{V})$  and  $\mathbf{Q}(\mathbf{V})$  represent currents and charges of the nonlinear subnetwork,  $\mathbf{I}_{ss}$  represents sources,  $\mathbf{Y}_{\text{ANN,EM}}$  represents admittance matrix corresponding to the EM-based ANN model, and  $\boldsymbol{\Omega}$  is an angular frequency matrix.

For a two-port passive component,  $\mathbf{Y}_{\text{ANN,EM}}$  are supplied by either direct frequency domain or SSE-NN or EC-SSE-NN neural models. Evaluation of our EC-SSE-NN model involves two steps. First,  $Y$ -parameter approximations from the EC sub-model are computed. Second, the differences  $\Delta\mathbf{Y}$  that account for the missing EM effects provided by the SSE-NN sub-model are added to the  $Y$ -parameter approximations to obtain  $\mathbf{Y}_{\text{ANN,EM}}$ . It is to be noted that solving the HB circuit (13) by incorporating EM-based neural models is much faster than directly using CPU-intensive EM simulations.

### B. Time-Domain or Transient Nonlinear Simulation

Time-domain or transient simulation is important for high-speed circuit design such as signal integrity analysis and optimization [17]. Nonlinear simulation equation for a circuit  $\pi$  with lumped linear components and nonlinear devices is

$$\mathbf{C}_\pi \dot{\mathbf{v}}(t) + \mathbf{G}_\pi \mathbf{v}(t) + \mathbf{F}(\mathbf{v}) = \mathbf{i}_s(t) \quad (14)$$

where  $\mathbf{v}(t)$  is typically a vector of node voltages,  $\mathbf{C}_\pi$  and  $\mathbf{G}_\pi$  are constant matrices with elements determined by lumped components,  $\mathbf{F}$  is a vector of functions representing currents in nonlinear devices, and  $\mathbf{i}_s(t)$  represent sources. In this section, a more general nonlinear circuit that contains lumped linear components, nonlinear devices, and additional linear subnetworks (e.g., EM-based SSE-NN, or EC-SSE-NN models of passive

components) is considered. The new time-domain nonlinear circuit equations are

$$\mathbf{C}_\pi \dot{\mathbf{v}}(t) + \mathbf{G}_\pi \mathbf{v}(t) + \mathbf{F}(\mathbf{v}(t)) + \sum_{i=1}^{N_{\text{ANN}}} (\mathbf{P}_i \mathbf{C}_i \mathbf{v}_i(t) + \mathbf{P}_i \mathbf{D}_i \mathbf{P}_i^T \mathbf{v}(t)) = \mathbf{i}_s(t) \quad (15)$$

and

$$\dot{\mathbf{v}}_i(t) = \mathbf{A}_i \mathbf{v}_i(t) + \mathbf{B}_i \mathbf{P}_i^T \mathbf{v}(t), \quad i = 1, 2, \dots, N_{\text{ANN}} \quad (16)$$

where  $N_{\text{ANN}}$  is number of SSE-NN or EC-SSE-NN models representing the EM-based passive components,  $\mathbf{P}_i$  is an incidence matrix containing  $\pm 1$ 's and 0's that maps the terminal voltages of the SSE-NN/EC-SSE-NN model into the node space of circuit  $\pi$ , and  $\mathbf{v}_i(t)$  are newly added state variables due to the  $i$ th SSE-NN/EC-SSE-NN model. Matrices  $\mathbf{A}_i$ ,  $\mathbf{B}_i$ ,  $\mathbf{C}_i$ , and  $\mathbf{D}_i$  are state-space matrices, which are formulated by arranging the coefficients  $\tilde{\mathbf{p}}_{\text{TF}}$  estimated by  $\mathbf{h}_{\text{ANN}}$  of the  $i$ th SSE-NN/EC-SSE-NN model into a format specific to our choice of the TFs as (17)–(19), shown at the bottom of this page, and

$$\mathbf{D}_i = \begin{bmatrix} b_{11}^{(n)} & b_{21}^{(n)} \\ b_{21}^{(n)} & b_{22}^{(n)} \end{bmatrix}_{2 \times 2}. \quad (20)$$

Lumped elements in the EC part of the proposed EC-SSE-NN models are supplied to  $\mathbf{C}_\pi$  and  $\mathbf{G}_\pi$  matrices of (15). Equation (15) and (16) ensure a complete time-domain description of the nonlinear circuit under consideration including both neural (SSE-NN and EC-SSE-NN) and non-neural subnetworks.

## VI. DEMONSTRATION EXAMPLES

### A. EM-Based Optimization of a Three-Stage Amplifier Circuit

In this example, we develop EM-based neural models of embedded resistors and capacitors and apply them to frequency-domain optimization of a three-stage amplifier circuit, as shown

$$\mathbf{A}_i = \begin{bmatrix} 0 & 1 & 0 & \dots & 0 & 0 & 0 & \dots & 0 & 0 \\ 0 & 0 & 1 & \dots & 0 & 0 & 0 & \dots & 0 & 0 \\ \vdots & \vdots & \vdots & \ddots & 0 & \vdots & \vdots & \ddots & \vdots & \vdots \\ -a^{(0)} & -a^{(1)} & -a^{(2)} & \dots & -a^{(n-1)} & 0 & 0 & \dots & 0 & 0 \\ 0 & 0 & \dots & 0 & 0 & 0 & 1 & 0 & \dots & 0 \\ 0 & 0 & \dots & 0 & 0 & 0 & 0 & 1 & \dots & 0 \\ \vdots & \vdots & \ddots & \vdots & \vdots & \vdots & \vdots & \vdots & \ddots & \vdots \\ 0 & 0 & \dots & 0 & 0 & -a^{(0)} & -a^{(1)} & -a^{(2)} & \dots & -a^{(n-1)} \end{bmatrix}_{2n \times 2n} \quad (17)$$

$$\mathbf{B}_i = \begin{bmatrix} 0 & 0 & \dots & 1 & 0 & 0 & \dots & 0 \\ 0 & 0 & \dots & 0 & 0 & 0 & \dots & 1 \end{bmatrix}_{2n \times 2}^T \quad (18)$$

$$\mathbf{C}_i = \begin{bmatrix} b_{11}^{(0)} - a^{(0)}b_{11}^{(n)} & \dots & b_{11}^{(n-1)} - a^{(n-1)}b_{11}^{(n)} & b_{21}^{(0)} - a^{(0)}b_{21}^{(n)} & \dots & b_{21}^{(n-1)} - a^{(n-1)}b_{21}^{(n)} \\ b_{21}^{(0)} - a^{(0)}b_{21}^{(n)} & \dots & b_{21}^{(n-1)} - a^{(n-1)}b_{21}^{(n)} & b_{22}^{(0)} - a^{(0)}b_{22}^{(n)} & \dots & b_{22}^{(n-1)} - a^{(n-1)}b_{22}^{(n)} \end{bmatrix}_{2 \times 2n} \quad (19)$$

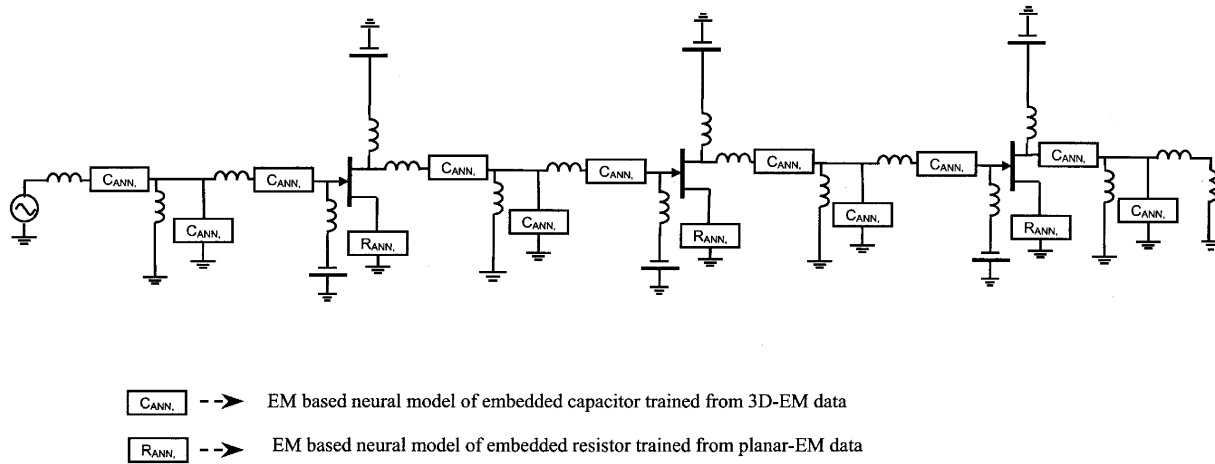


Fig. 6. Three-stage amplifier circuit in ADS showing EM-based ANN models incorporated into nonlinear circuit simulation to facilitate accurate and fast frequency-domain optimization of the circuit at high frequencies.

in Fig. 6. Frequency-domain neural models of the embedded passives are developed using the standard approach described in Section II. The embedded resistor neural model has five inputs, i.e.,  $\mathbf{x} = [L_R \ W_R \ \rho \ \varepsilon_{r,\text{sub}} \ \omega]^T$ , where the parameters in  $\mathbf{x}$  are defined in Fig. 1. The model has four output parameters, i.e.,  $\mathbf{y} = [RS_{11} \ IS_{11} \ RS_{21} \ IS_{21}]^T$ , since the resistor used has a symmetric structure. A SONNET<sup>1</sup> driver based on the proposed automatic mechanism for efficient EM data generation is developed. In this example, we used a grid sampling scheme [3] for generating EM data in the five-dimensional space of  $\mathbf{x}$ . For example, if we use seven grid points in each geometrical/physical input dimension (i.e.,  $L_R$ ,  $W_R$ ,  $\rho$ ,  $\varepsilon_{r,\text{sub}}$ ) and 24 points in frequency  $\omega$ , the total number of samples will be in the order of 50 000–60 000. A set of models was trained for different ranges of input parameters with an average number of training samples being 55 000 [23]. The average amount of time for data generation and model training is 12 h. The embedded capacitor neural model has five inputs, i.e.,  $\mathbf{x} = [L_C \ T_C \ \varepsilon_{r,\text{cap}} \ \varepsilon_{r,\text{sub}} \ \omega]^T$ , where the parameters in  $\mathbf{x}$  are defined in Fig. 7. The model has six output parameters, i.e.,  $\mathbf{y} = [RS_{11} \ IS_{11} \ RS_{21} \ IS_{21} \ RS_{22} \ IS_{22}]^T$ . An HFSS-driver is developed for automatically driving the Ansoft-HFSS simulator.<sup>2</sup> A set of capacitor neural models was trained with average amount of training data being 65 000 [23]. Data generation and model training took an average of 26 h. The trained neural networks can be subsequently used as fast models of resistors and capacitors representing the  $S$ -parameter variations with respect to changes in geometrical/physical input parameters.

These models are used to provide EM-level effects of the embedded passive components for large-signal HB simulation and optimization of the three-stage amplifier. The amplifier circuit consists of passive components such as embedded resistors and embedded capacitors, and active devices. The FETs in the circuit are replaced by large-signal models through an adjoint neural-network method [24] implemented in ADS.<sup>3</sup> The

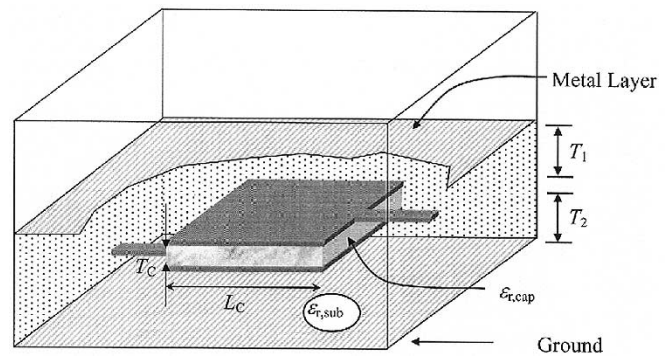


Fig. 7. Geometrical structure of embedded capacitor in multilayer PCBs. Various ANN approaches including the proposed EC-SSE-NN are used to develop neural models of the capacitor from EM data.

$Q$ -point of the amplifier circuit is fixed to be  $V_{DS} = 3.2$  V and  $V_{GS} = -0.6$  V, and EM-based frequency-domain optimization of the circuit is carried out using HB in ADS. The use of neural models allows geometrical/physical parameters of the embedded passives to be included as optimization variables. During circuit optimization, every time the geometrical parameters change, neural models are recalled to provide quick estimation of the EM behavior of passive components. In this way, repetitive and expensive executions of detailed EM simulations are avoided. The results of amplifier optimization using our EM-based neural models are shown in Fig. 8 and compared with that using ideal lumped models, and that using empirical/equivalent-circuit library models in the simulator. Results from ideal and empirical models are closer to our EM-based results at low frequencies, but at high frequencies, they differ, and EM-based solutions are more important. Figs. 9 and 10 show the frequency- and time-domain solutions of the amplifier circuit using our EM-based neural models. This example shows that neural networks make it much easier to incorporate EM effects into nonlinear HB simulation and optimization, which otherwise would be difficult to achieve with direct EM simulators. The example also illustrates that effects of multiple EM simulators such as ANSOFT-HFSS for 3-D-EM and SONNET for planar EM, can all be made accessible and optimizable in a

<sup>1</sup>SONNET, ver.7.0, Sonnet Software Inc., Liverpool, NY, 2001.

<sup>2</sup>HFSS, ver. 8.0, Ansoft Corporation, Pittsburgh, PA, 2001.

<sup>3</sup>ADS, ver. 1.5, Agilent Technol., Palo Alto, CA 2001.

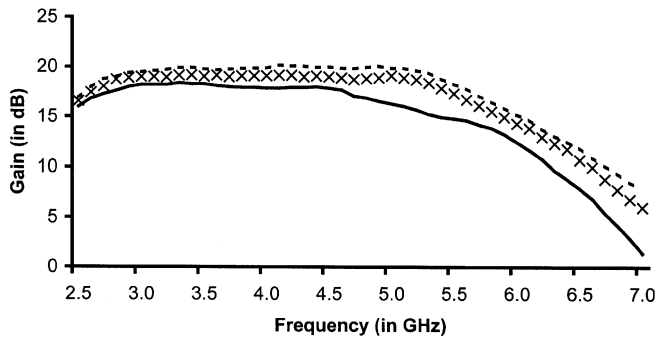


Fig. 8. Gain of the optimized three-stage amplifier circuit when passive components are replaced by ideal lumped models (—), empirical/equivalent-circuit library models (xxx), and EM-based ANN models (—).

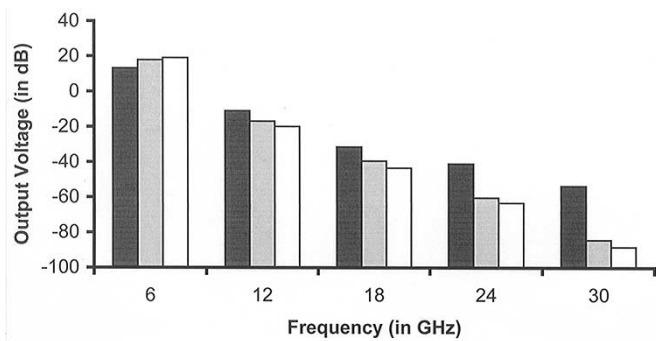


Fig. 9. Large-signal HB solution of output voltage spectrum of the optimized three-stage amplifier circuit when passive components are replaced by ideal lumped models (□), empirical/equivalent-circuit library models (■), and EM-based ANN models (■).

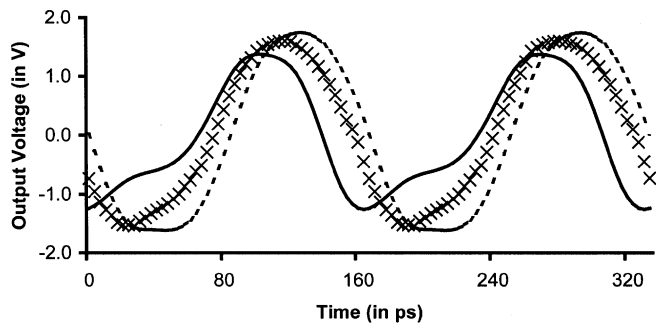


Fig. 10. Large-signal HB solution of output voltage waveform of the optimized three-stage amplifier circuit when passive components are replaced by ideal lumped models (—), empirical/equivalent-circuit library models (xxx), and EM-based ANN models (—). Nonlinear characteristics of the circuit are present in the EM-based solution.

high-level nonlinear HB environment such as ADS because of the use of neural-network formulations. This aspect is summarized in Fig. 11.

### B. Time-Domain Optimization With Power Distribution Model in Multilayer Printed Circuits

A multilayer PCB often contains power planes distributing the dc supply to various components. At high signal speed, the power plane is not an ideal conductor and the high-frequency effects need to be considered [25], [26]. In this example, we

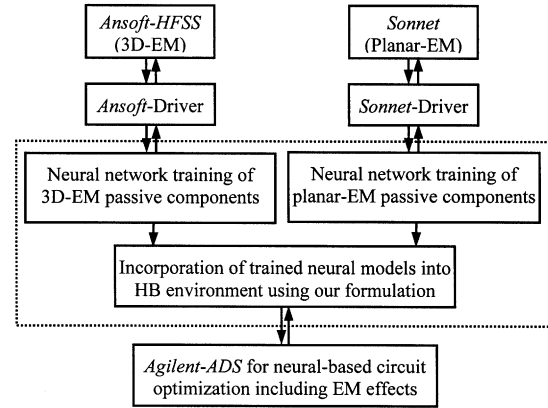


Fig. 11. Incorporation of various EM-simulator-based neural models on to a single platform through neural-based methodologies used in the amplifier example.

illustrate physical/geometrical-based time-domain circuit optimization including power-plane effects. First, we develop neural models to learn from EM data of power plane versus geometrical parameters. Second, these neural models are used in circuit optimization.

Fig. 12 shows a power plane supplying a dc source to four IC packages. We represent power-plane effects of an IC connection with the power supply by a corresponding neural model [27]. Let  $(X, Y)$  representing the coordinates of the dc source ( $V_{DC}$ ) be the reference point. Let coordinates  $(dX_i, dY_i)$  represent geometrical location of the connection of the  $i$ th IC to the power plane, relative to the reference point. The position of the  $i$ th IC is given by

$$X_i = X + dX_i \quad (21)$$

and

$$Y_i = Y + dY_i. \quad (22)$$

The input parameters to our power-plane neural model include  $X$ ,  $Y$ ,  $dX_i$ , and  $dY_i$ . Varying the reference point and the relative IC placements, data is generated at different frequencies using EM simulation.<sup>4</sup> An SSE-NN model is developed where a three-layer MLP neural network is trained to learn the TF coefficient versus geometry relationships using the NeuroModeler program.<sup>5</sup> This power-plane neural model is then used for the optimization of transient responses in a 4-bit board-level interconnect circuit. The circuit consists of a power plane and several ICs, as shown in Fig. 12, with nonlinear buffers in all IC terminal pins. The SSE-NN neural model for the power plane is used four times with common values of  $(X, Y)$  and different values of  $(dX_i, dY_i)$  to represent connection of four ICs on the same power plane. Fig. 13 shows schematics of the board-level interconnect circuit including nonlinear buffers from the IC packages. The objective of optimization is to reduce signal distortion and crosstalk in the presence of power planes. Parameters that are changed during optimization include  $(X, Y)$ ,  $(dX_i, dY_i)$ ,  $i = 1, 2, 3$ , and 4, which also implies that the lengths ( $L_{T1}, L_{T2}, L_{T3}$ ) of transmission lines change accordingly. During optimization,

<sup>4</sup>SIwave, ver. 1.1, Ansoft Corporation, Pittsburgh, PA, 2002.

<sup>5</sup>Q. J. Zhang, NeuroModeler, ver. 1.2, Dept. Electron., Carleton Univ., Ottawa, ON, Canada, 2001.

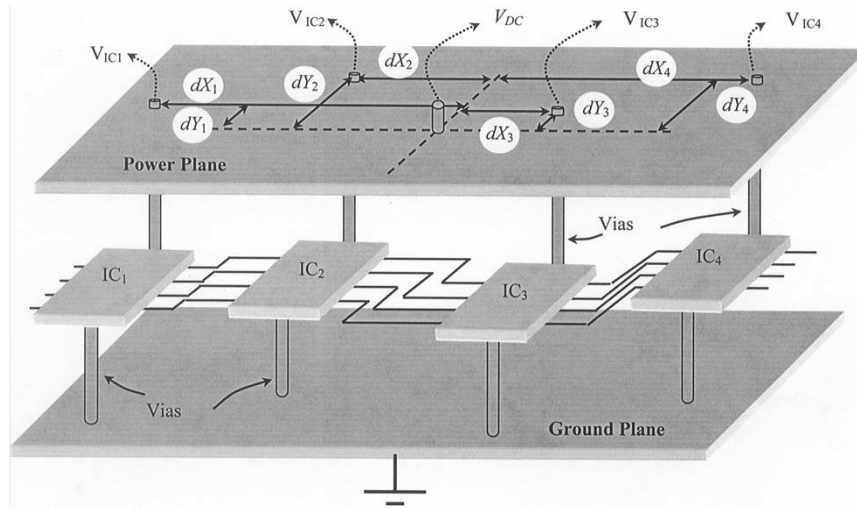


Fig. 12. Physical representation of the 4-bit board-level interconnect circuit consisting of a power plane and four ICs. In our formulation, coordinates of the dc source ( $V_{DC}$ ) are defined as the reference point.

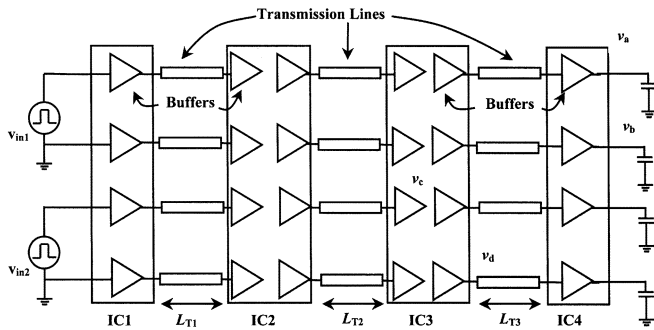


Fig. 13. Schematic of the board-level interconnect circuit with four ICs to be connected to the power plane of Fig. 12. Signal integrity optimization of the circuit is carried out including geometrical parameters as optimization variables using power-plane neural models.

every time any of these variables change, the circuit responses including power-plane effects need to be recomputed, and fast neural models are suited for this purpose. A trapezoidal signal with 0.1-ns rise/fall time and 2-ns duration is used as the excitation signal. Specifications on the distortion in signals  $v_a$  and  $v_c$  and on the crosstalk in  $v_b$  and  $v_d$  were formulated following [17]. Optimization constraints were added such that each transmission-line length should be at least 1 cm, and the total length of the three transmission-line sections should be 6.4 cm. After optimization, the distortions of  $v_a$  and  $v_c$  are reduced from up to 5-V deviation from ideal down to within 0.6-V deviation, as shown in Fig. 14. The peak-to-peak crosstalk noise in  $v_b$  and  $v_d$  are reduced from 0.18 V down to 0.07 V. This example demonstrates that time-domain circuit optimization including geometrical variables of power-plane connections can be achieved through the use of neural-network modeling of the power plane.

### C. EM-Based Embedded Passive Modeling Using EC-SSE-NN and Signal Integrity Optimization of a High-Speed VLSI Interconnect Circuit

In this example, we demonstrate time-domain EM-based models of embedded passives using the proposed EC-SSE-NN approach and their use in EM-based signal integrity optimiza-

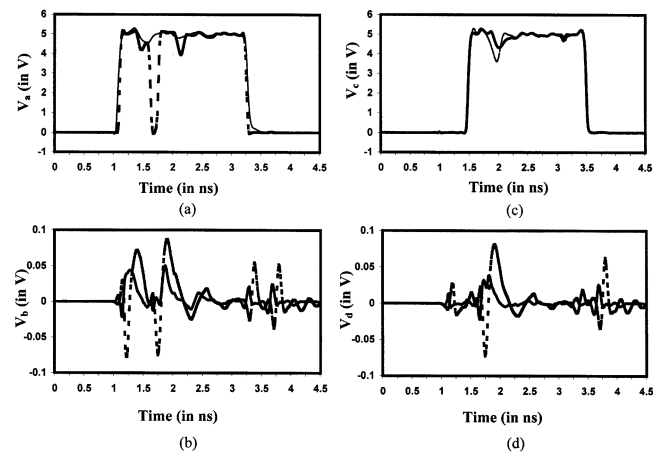


Fig. 14. Time-domain responses of the board-level interconnect circuit with power-plane neural models before optimization (—) and after optimization (---). (a) Signal  $v_a$ . (b) Crosstalk  $v_b$ . (c) Signal  $v_c$ . (d) Crosstalk  $v_d$ .

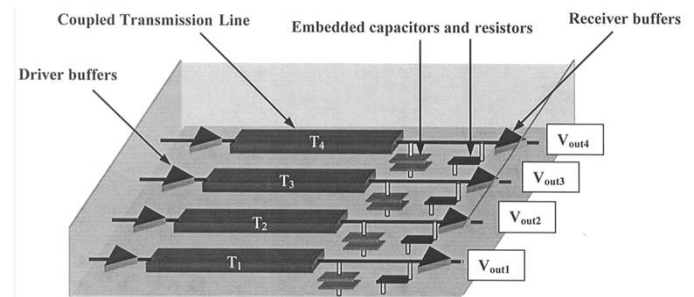


Fig. 15. 3-D illustration of a multilayer circuit with embedded resistors and capacitors, coupled transmission lines, and nonlinear terminations considered for EM-based signal integrity analysis using ANN approaches.

tion of a high-speed VLSI interconnect circuit shown in Fig. 15. The overall interconnect circuit consists of transmission lines, embedded resistors, and capacitors, and is terminated with nonlinear buffers. EM-based models of embedded passive components are important for high-speed PCB design [23], [28], [29]. First, we develop EM-based neural models of embedded resistors and capacitors employing proposed EC-SSE-NN approaches. Second, these EC-SSE-NN models are used for

carrying out optimization of the overall nonlinear circuit in the time domain including geometrical parameters as variables.

#### D. Time-Domain EC–SSE–NN Modeling of Embedded Resistors

EC–SSE–NN models of the embedded resistor shown in Fig. 1 are developed. Length ( $L_R$ ) and width ( $W_R$ ) are used as model inputs  $\mathbf{x}$ , and real and imaginary parts of  $S_{11}$  and  $S_{21}$  data are used to train the model. A SONNET-driver program implementing the proposed automatic mechanism is used for efficient generation of EM data using SONNET. The lumped circuit in Fig. 2(a) is used as the EC sub-model exploiting empirical functions, e.g.,

$$R = \frac{L_R}{W_R} \rho \quad (23)$$

$$C_1 = C_2 = \varepsilon_o \frac{L_R \cdot W_R}{T_1 \cdot T_2} (T_1 + T_2) \varepsilon_{r,\text{sub}} \quad (24)$$

where  $\rho$  is resistivity per square,  $T_1$  and  $T_2$  are the distances between the resistor and the two metal planes, and  $\varepsilon_{r,\text{sub}}$  represents substrate dielectric constant. TFs of different orders ( $n = 2, 3$ , and 4) are used to fit admittance mismatch  $\Delta Y$  between that of the EM data and the EC sub-model. PE optimization was performed in ADS with a gradient-based method. The two geometrical variables  $L_R$  (30–60 mil with a step of 2.5 mil) and  $W_R$  (6–12 mil with a step of 2 mil) necessitated 52 PEs over a frequency ranges of interest (0.1–1 GHz with a step of 0.1 GHz and 1–16 with a step 1 GHz). Second-order TFs are used in the SSE–NN part of the model to represent the difference. Optimal values of coefficients in the TFs of (5) are determined for each geometrical configuration. A three-layer MLP with two input neurons, 12 hidden neurons, and eight output neurons, is trained to learn the relationship between  $\mathbf{x}$  and  $\mathbf{p}_{\text{TF}}$  using sample pairs  $(\mathbf{x}_k, \mathbf{p}_{\text{TF},k})$ . The trained EC–SSE–NN model is tested in both the frequency and time domains using independent EM simulations and transient data of the embedded resistor. A good agreement between  $S$ -parameters from a full-wave EM and EC–SSE–NN model is achieved, as illustrated in Fig. 16. For comparison purpose, we also trained several SSE–NN and EC–SSE–NN models using different orders of the TF and compared the results in Table I. For a given accuracy, the EC–SSE–NN uses fewer EM data than pure SSE–NN. To confirm the validity of the time-domain solution of our EC–SSE–NN, we used a fast Fourier transform (FFT) on original EM data to obtain time-domain test data. Such EM-based time-domain responses agree with EC–SSE–NN model responses, as shown in Fig. 17, confirming validity of our EC–SSE–NN model.

#### E. Time-Domain EC–SSE–NN Modeling of Embedded Capacitors

EC–SSE–NN models of the square embedded capacitor shown in Fig. 7 are developed. Inputs  $\mathbf{x}$  include length ( $L_C$ ) and dielectric constant ( $\varepsilon_{r,\text{cap}}$ ), and two-port  $S$ -parameter data is used to train the model. A lumped EC of the capacitor, shown in Fig. 2(b), is used as an EC sub-model, where the empirical functions for  $C_1$  and  $C_2$  are defined similarly to (24), the function for  $C_C$  is defined similarly to (24) with  $T_1$  and  $T_2$ ,  $\varepsilon_{r,\text{sub}}$  is

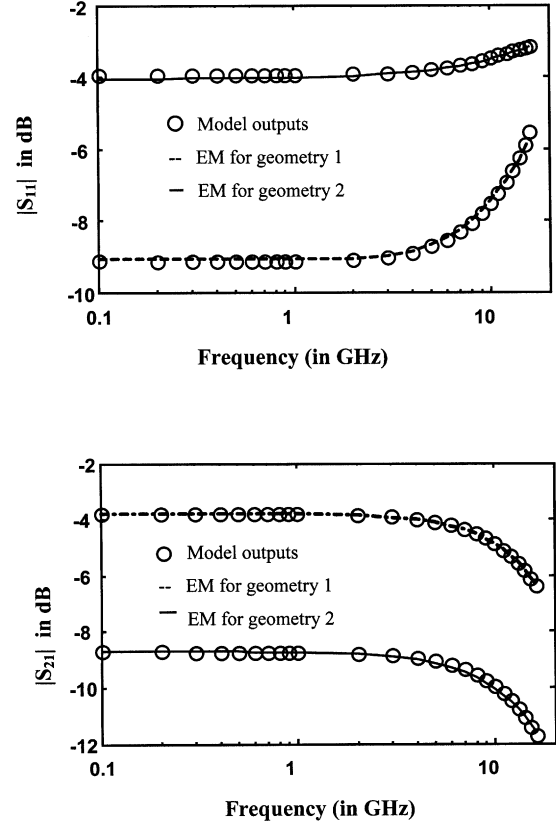


Fig. 16. Comparison of  $S$ -parameters from an EC–SSE–NN model and EM data for two different sizes of the embedded resistor.

TABLE I  
MODEL ACCURACY COMPARISON BETWEEN SSE–NN AND EC–SSE–NN MODELS FOR THE EMBEDDED RESISTOR. EC–SSE–NN MODELS ACHIEVE BETTER ACCURACIES WITH THE SAME AMOUNT OF EM TRAINING DATA

Model order	Average test error of SSE–NN model			Average test error of proposed EC–SSE–NN model		
	Number of EM training data	Number of EM training data	Number of EM training data	Number of EM training data	Number of EM training data	Number of EM training data
$(n)$	600	1200	1500	600	1200	1500
2	3.96%	1.59%	0.89%	1.05%	0.68%	0.52%
3	4.33%	1.12%	0.71%	0.87%	0.54%	0.49%
4	7.30%	2.38%	1.13%	3.11%	1.78%	0.98%

replaced by  $T_C$ ,  $T_C$ , and  $\varepsilon_{r,\text{cap}}$ , respectively, and  $L$  are defined following [29]. To generate training data for the embedded square capacitor, the input parameters are varied:  $L_C$  (26–40 mil, step 2 mil) and  $\varepsilon_{r,\text{cap}}$  (12.5–22.5, step 5). For each set of  $L_C$  and  $\varepsilon_{r,\text{cap}}$  values, a frequency sweep (0.1–1 GHz, step 0.1 GHz; 1–16, step 1 GHz) is used to generate the  $S$ -parameters. An HFSS-driver macro-program implementing the proposed automatic mechanism is used for efficient generation of EM data using Ansoft-HFSS. PE has been performed 24 times in

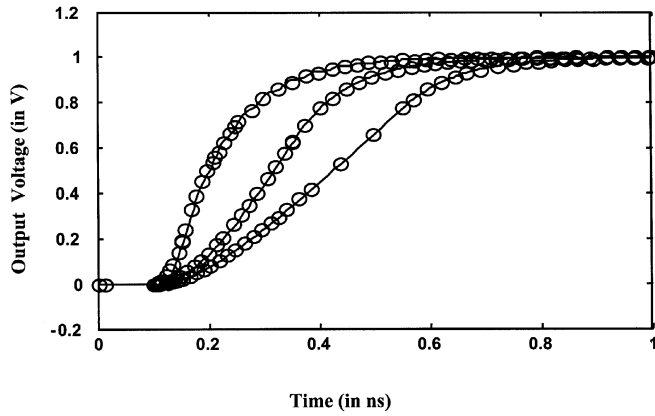


Fig. 17. Comparison of transient responses of an EC-SSE-NN model (○) and EM data (—) for the embedded resistor. Three step waveform inputs with different rise-time (0.05, 0.25, and 0.45 ns) have been considered.

TABLE II

MODEL ACCURACY COMPARISON BETWEEN SSE-NN MODELS AND PROPOSED EC-SSE-NN MODELS FOR THE EMBEDDED CAPACITOR. THE EC-SSE-NN MODELS ACHIEVE BETTER ACCURACIES WITH THE SAME AMOUNT OF EM TRAINING DATA AS SSE-NN

Model order	Average test error of SSE-NN model			Average test error of proposed EC-SSE-NN model		
	Number of EM training data	Number of EM training data	Number of EM training data	Number of EM training data	Number of EM training data	Number of EM training data
(n)	360	720	900	360	720	900
2	4.76%	2.20%	1.28%	1.15%	0.57%	0.45%
3	3.89%	1.67%	0.93%	0.91%	0.41%	0.32%
4	6.34%	2.57%	1.43%	3.68%	2.06%	1.17%

ADS to optimize the corresponding coefficients within the entire frequency range. Eight coefficients in  $\mathbf{p}_{TF}$  from TF (5) are used in the second-order SSE formulas. A three-layer MLP with two input neurons, 12 hidden neurons, and eight output neurons, is trained to learn the relationship between  $\mathbf{x}$  and  $\mathbf{p}_{TF}$  using sample pairs  $(\mathbf{x}_k, \mathbf{p}_{TF,k})$ . A good agreement between  $S$ -parameters from a full-wave EM and EC-SSE-NN model is achieved, as shown in Table II and Fig. 18. The time-domain response of the EC-SSE-NN model matches well with that using FFT of the detailed EM simulation, as shown in Fig. 19. For comparison purpose, we also trained several SSE-NN and EC-SSE-NN models with different orders of the TF, and compared the results in Table II. This table shows that the proposed EC-SSE-NN approach utilizing existing knowledge achieves increased model accuracy compared to pure SSE-NN while using the same amount of training data. Alternatively, EC-SSE-NN can be used to achieve the same accuracy as SSE-NN with fewer training data.

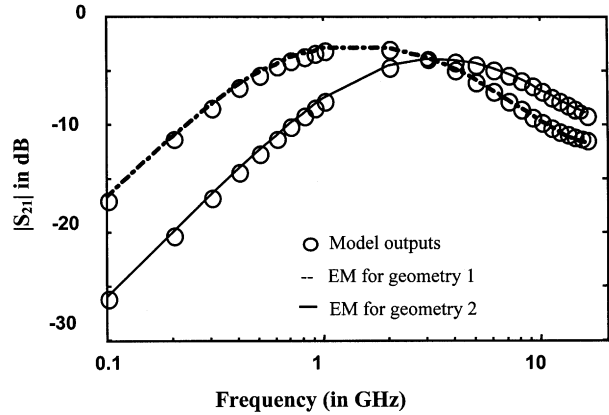
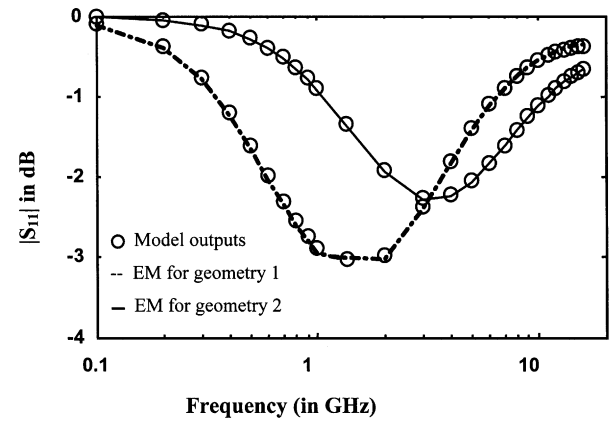


Fig. 18. Comparison of  $S$ -parameters from EC-SSE-NN model and EM data for two different sizes of the embedded capacitor.

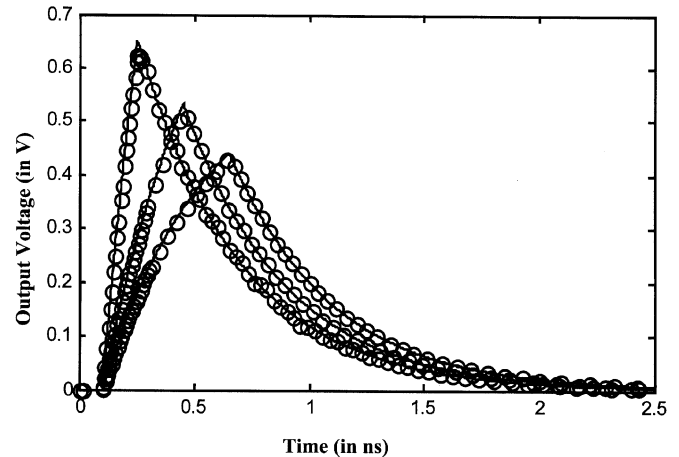


Fig. 19. Comparison of transient responses of EC-SSE-NN model (○) and EM data (—) for the embedded capacitor. Three step waveform inputs with different rise-time (0.15, 0.20, and 0.55 ns) have been considered.

#### F. Signal Integrity Analysis Including Geometrical/Physical Parameters

To demonstrate EM-based nonlinear circuit optimization in the time domain, we incorporated our EC-SSE-NN models of embedded passives into HSPICE<sup>6</sup> and performed signal integrity simulation and optimization on the interconnect circuit of Fig. 15 including geometrical/physical parameters as

<sup>6</sup>HSPICE, ver. 2001.2, Synopsys Inc., Mountain View, CA, 2001.

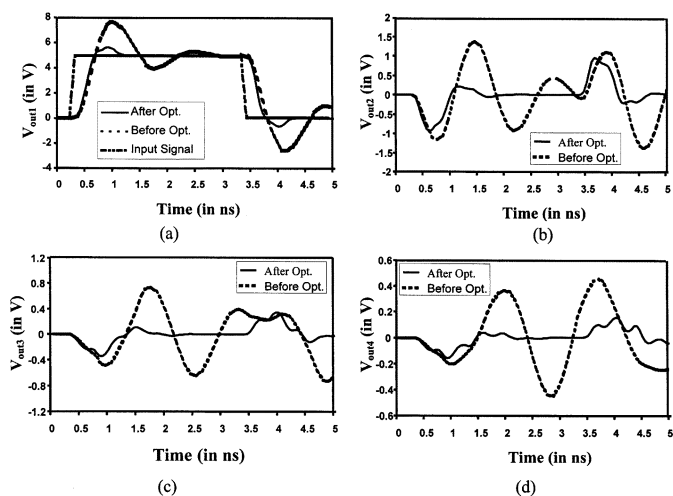


Fig. 20. Comparison of: (a) signal and (b)–(d) crosstalk of the high-speed signal integrity VLSI circuit including EM-based embedded resistors, capacitors, and nonlinear terminations before optimization and after EM-based optimization using EC–SSE–NN models.

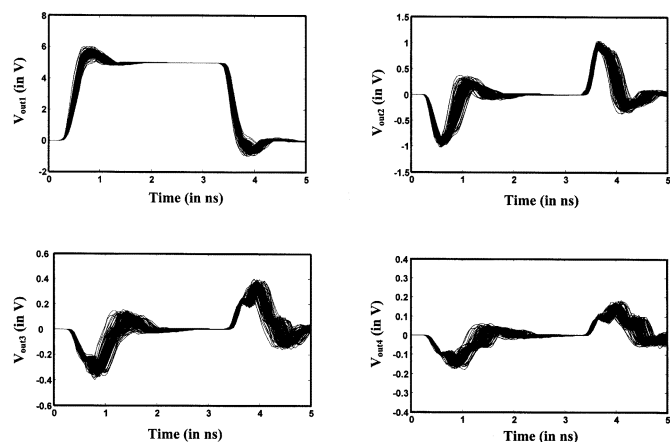


Fig. 21. Results showing 500 Monte Carlo time-domain responses of the optimized signal integrity circuit including embedded resistors, capacitors, and nonlinear terminations. The circuit is optimized using EM-based EC–SSE–NN models of embedded passive components.

variables. A high-speed digital source with 0.1-ns rise time is used to drive the first interconnection in the nonlinear circuit. Length of the four coupled transmission lines is 2.78 cm. The objective of optimization is to decrease overshoot and reduce time delay. During optimization, the EC–SSE–NN models allow repetitive adjustment of  $L_R$ ,  $W_R$ ,  $L_C$ , and  $\epsilon_{r,cap}$  with computational speeds much faster than detailed EM models. A total of 44 iterations are used and the time taken for EM-based optimization using EC–SSE–NN models is 3.50 min. Signal and crosstalk before and after optimization are compared in Fig. 20. We also performed statistical analysis of the circuit using EC–SSE–NN models. Monte Carlo responses of 500 circuits with different geometrical/physical parameters are shown in Fig. 21. Simulation time for Monte Carlo analysis of the entire circuit using our EC–SSE–NN models is a mere 7.75 min, as compared to over 5 h required by the EM simulator

for Monte Carlo analysis of just the passive components. This example shows that the proposed work allows the SPICE environment, which previously does not have a full-wave EM feature, now be extended to EM-based design with geometrical dimensions and physical properties as variables for EM-based time-domain CAD.

## VII. CONCLUSIONS

In this paper, ANN approaches to EM-based modeling and optimization have been presented. The EM-based neural models have been formulated to enable EM behaviors of passive components to interact with nonlinear behaviors of active devices to facilitate nonlinear circuit design in the frequency and time domains. A novel EC–SSE–NN approach combining existing knowledge in the form of ECs, together with SSEs and neural networks, has been proposed for developing EM-based time-domain models to be used in nonlinear circuit optimization. The presented models possess advantages of compactness, ease of implementation, and applicability to the frequency and time domains. Neural networks, with combined advantages of speed and accuracy, coupled with the ability to learn and generalize a variety of EM component and circuit behaviors, provide a powerful alternative vehicle for EM-based modeling and optimization of high-frequency/high-speed electronic circuits.

## ACKNOWLEDGMENT

Author Q. J. Zhang wish to thank R. Sheffield, H. Feyzbakhsh, H. Kwong, and L. Marcanti, all of Nortel Networks, Ottawa, ON, Canada, for many discussions on embedded passives, and for their support and collaboration of this research.

## REFERENCES

- [1] M. B. Steer, J. W. Bandler, and C. M. Snowden, "Computer-aided design of RF and microwave circuits and systems," *IEEE Trans. Microwave Theory Tech.*, vol. 50, pp. 996–1005, Mar. 2002.
- [2] K. C. Gupta, "Emerging trends in millimeter-wave CAD," *IEEE Trans. Microwave Theory Tech.*, vol. 46, pp. 747–755, June 1998.
- [3] Q. J. Zhang and K. C. Gupta, *Neural Networks for RF and Microwave Design*. Norwood, MA: Artech House, 2000.
- [4] P. Burrascano, S. Fiori, and M. Mongiardo, "A review of artificial neural networks applications in microwave computer-aided design," *Int. J. RF Microwave Computer-Aided Eng.*, vol. 9, pp. 158–174, 1999.
- [5] J. W. Bandler, M. A. Ismail, J. E. Rayas-Sanchez, and Q. J. Zhang, "Neuromodeling of microwave circuits exploiting space-mapping technology," *IEEE Trans. Microwave Theory Tech.*, vol. 47, pp. 2417–2427, Dec. 1999.
- [6] V. K. Devabhaktuni, M. C. E. Yagoub, and Q. J. Zhang, "A robust algorithm for automatic development of neural network models for microwave applications," *IEEE Trans. Microwave Theory Tech.*, vol. 49, pp. 2282–2291, Dec. 2001.
- [7] V. K. Devabhaktuni, C. X. F. Wang, and Q. J. Zhang, "Robust training of microwave neural models," *Int. J. RF Microwave Computer-Aided Eng.*, vol. 12, pp. 109–124, 2002.
- [8] A. Veluswami, M. S. Nakhla, and Q. J. Zhang, "The application of neural networks to EM-based simulation and optimization of interconnects in high-speed VLSI circuits," *IEEE Trans. Microwave Theory Tech.*, vol. 45, pp. 712–723, May 1997.
- [9] F. Wang and Q. J. Zhang, "Knowledge-based neural models for microwave design," *IEEE Trans. Microwave Theory Tech.*, vol. 45, pp. 2333–2343, Dec. 1997.

- [10] P. M. Watson and K. C. Gupta, "EM-ANN models for microstrip vias and interconnects in dataset circuits," *IEEE Trans. Microwave Theory Tech.*, vol. 44, pp. 2495–2503, Dec. 1996.
- [11] —, "Design and optimization of CPW circuits using EM-ANN models for CPW components," *IEEE Trans. Microwave Theory Tech.*, vol. 45, pp. 2515–2523, Dec. 1997.
- [12] G. L. Creech, B. J. Paul, C. D. Lesniak, T. J. Jenkins, and M. C. Calcaterra, "Artificial neural networks for fast and accurate EM-CAD of microwave circuits," *IEEE Trans. Microwave Theory Tech.*, vol. 45, pp. 794–802, May 1997.
- [13] A. H. Zaabab, Q. J. Zhang, and M. S. Nakhla, "A neural network modeling approach to circuit optimization and statistical design," *IEEE Trans. Microwave Theory Tech.*, vol. 43, pp. 1349–1358, June 1995.
- [14] P. M. Watson, K. C. Gupta, and R. L. Mahajan, "Applications of knowledge-based artificial neural network modeling to microwave components," *Int. J. RF Microwave Computer-Aided Eng.*, vol. 9, pp. 254–260, 1999.
- [15] S. Lum, M. Nakhla, and Q. J. Zhang, "Sensitivity analysis of lossy coupled transmission lines with nonlinear terminations," *IEEE Trans. Microwave Theory Tech.*, vol. 42, pp. 607–615, Apr. 1994.
- [16] X. Ding, J. Xu, M. C. E. Yagoub, and Q. J. Zhang, "A new modeling approach for embedded passives exploiting state space formulation," in *Proc. Eur. Microwave Conf.*, Milan, Italy, 2002, pp. 229–232.
- [17] Q. J. Zhang, S. Lum, and M. S. Nakhla, "Minimization of delay and crosstalk in high-speed VLSI interconnects," *IEEE Trans. Microwave Theory Tech.*, vol. 40, pp. 1555–1563, July 1992.
- [18] Q. J. Zhang, F. Wang, and M. S. Nakhla, "Optimization of high-speed VLSI interconnects: A review," *Int. J. Microwave Millimeter-Wave Computer-Aided Eng.*, vol. 7, pp. 83–107, 1997.
- [19] J. M. Williamson, M. Nakhla, Q. J. Zhang, and P. D. van der Puije, "Ground noise minimization in integrated circuit packages through pin assignment optimization," *IEEE Trans. Comput., Packag., Manufact. Technol.*, vol. 19, pp. 361–371, May 1996.
- [20] C. P. Coelho, J. R. Phillips, and L. M. Silveira, "A convex programming approach to positive real rational approximation," in *Proc. Int. Conf. Computer-Aided Design*, San Jose, CA, 2001, pp. 245–251.
- [21] V. Rizzoli and A. Neri, "State of the art and present trends in nonlinear microwave CAD techniques," *IEEE Trans. Microwave Theory Tech.*, vol. 36, pp. 343–365, Feb. 1988.
- [22] J. W. Bandler, R. M. Biernacki, Q. Cai, S. H. Chen, and P. A. Grobely, "Integrated harmonic balance and electromagnetic optimization with geometry capture," in *IEEE MTT-S Int. Microwave Symp. Dig.*, Orlando, FL, 1995, pp. 793–796.
- [23] Q. J. Zhang, M. C. E. Yagoub, X. Ding, D. Goulette, R. Sheffield, and H. Feyzbakhsh, "Fast and accurate modeling of embedded passives in multi-layer printed circuits using neural network approach," in *Electronic Components and Technology Conf.*, San Diego, CA, 2002, pp. 700–703.
- [24] J. Xu, M. C. E. Yagoub, R. Ding, and Q. J. Zhang, "Exact adjoint sensitivity analysis for neural based microwave modeling and design," in *IEEE MTT-S Int. Microwave Symp. Dig.*, Phoenix, AZ, 2001, pp. 1015–1018.
- [25] X. Xie and J. L. Prince, "Frequency response characteristics of reference plane effective inductance and resistance," *IEEE Trans. Adv. Packag.*, vol. 22, pp. 221–229, May 1999.
- [26] R. Mittra, S. Chebolu, and W. D. Becker, "Efficient modeling of power planes in computer packages using the finite difference time domain method," *IEEE Trans. Microwave Theory Tech.*, vol. 42, pp. 1791–1795, Sept. 1994.
- [27] B. Chattaraj, M. C. E. Yagoub, X. Ding, and Q. J. Zhang, "EM based optimization of microwave circuits by neural models and their application to power distribution and decoupling optimization," in *Proc. Eur. Microwave Conf.*, vol. 2, London, U.K., 2001, pp. 125–128.
- [28] R. Poddar and M. A. Brooke, "Accurate high speed empirically based predictive modeling of deeply embedded gridded parallel plate capacitors fabricated in a multilayer LTCC process," *IEEE Trans. Comput., Packag., Manufact. Technol.*, vol. 22, pp. 26–31, Feb. 1999.
- [29] K. L. Choi and M. Swaminathan, "Development of model libraries for embedded passives using network synthesis," *IEEE Trans. Circuits Syst.*, vol. 47, pp. 249–260, Apr. 2000.



**Xiaolei Ding (S'01)** received the B.Eng. degree in electrical engineering from the North China Institute of Technology, Taiyuan, China, in 1993, the M.A.Sc degree in electronics from Carleton University, Ottawa, ON, Canada, in 2002, and is currently working toward the Ph.D. degree in electronics at Carleton University.

His research interests include neural-network modeling of EM effects for embedded passives and their applications in CAD for high-speed/high-frequency circuits.

Mr. Ding was the recipient of the 2000–2002 Nortel Networks Scholarship and the 2003–2004 Ontario Graduate Student Scholarship in Science and Technology.



**Vijay K. Devabhaktuni (S'97)** received the B.Eng. degree in electrical and electronics engineering and M.Sc. degree in physics from the Birla Institute of Technology and Science, Pilani, Rajasthan, India, in 1996, and is currently working toward the Ph.D. degree in electronics at Carleton University, Ottawa, ON, Canada.

He is currently a Sessional Lecturer with the Department of Electronics, Carleton University. His research interests include ANNs, CAD methodologies for VLSI circuits, and RF and microwave modeling

techniques.

Mr. Devabhaktuni was the recipient of a 1999 Best Student Research Exhibit Award presented by Nortel Networks. He was a two-time recipient of the Ontario Graduate Scholarship for the 1999–2000 and 2000–2001 academic years presented by the Ministry of Education and Training, ON, Canada. He was the recipient of the 2001 John Ruptash Memorial Fellowship, which is awarded annually to an outstanding graduate student of the Faculty of Engineering, Carleton University. He was also the recipient of the 2001 Teaching Excellence Award in Engineering presented by the Carleton University Student's Association.



**Biswarup Chattaraj** was born in Calcutta, India, in 1978. He received the B.Tech degree in electronics and telecommunication from Nagpur University, Maharashtra, India, in 2000, the M.A.Sc degree in electronics from Carleton University, Ottawa, ON, Canada in 2002, and is currently working toward the Ph.D. degree in the electrical and computer engineering department from the University of Illinois, Chicago.

His research interest includes very large-scale integration (VLSI) CAD, circuit partitioning, placement, and routing, and design automation and reconfiguration of VLSI circuits.



**Mustapha C. E. Yagoub (M'96)** received the Diplôme d'Ingénieur degree in electronics and Magister degree in telecommunications from the Ecole Nationale Polytechnique, Algiers, Algeria, in 1979 and 1987, respectively, and the Ph.D. degree from the Institut National Polytechnique, Toulouse, France, in 1994.

He was with the Institute of Electronics, Université des Sciences et de la Technologie Houari Boumediène, Algiers, Algeria, initially as an Assistant from 1983 to 1991, and then as an Assistant Professor from 1994 to 1999. From 1999 to 2001, he was with the Department of Electronics, Carleton University, Ottawa, ON, Canada, where he was involved with neural-network applications in microwave areas. In 2001, he joined the School of Information Technology and Engineering (SITE), University of Ottawa, Ottawa, ON, Canada, where he is currently an Assistant Professor. His research interests include neural networks for microwave applications, CAD for linear and nonlinear microwave devices and circuits, and applied electromagnetics. He has authored over 80 publications on these topics in international journals and conferences. He coauthored *Conception de circuits linéaires et non linéaires micro-ondes* (Toulouse, France: Cépadués, 2000).

Dr. Yagoub is a member of the Association of Professional Engineers of the Province of Ontario, Canada.



**Makarand Deo** (S'02) received the B.E. degree from the Vishwakarma Institute of Technology, Pune University, Maharashtra, India, in 2000, the M. Tech. degree from the Indian Institute of Technology Bombay, Mumbai, India in 2002, and is currently working toward the Ph.D. degree from Carleton University, Ottawa, ON, Canada.

His research interests include ANNs, simulation and modeling of high-speed/high-frequency VLSI circuits, and modeling of nonlinear dynamic circuits and systems.



**Jianjun Xu** (S'00) was born in Liaoning, China, in August 1975. He received the B.Eng. degree in electrical and electronics engineering from Tianjin University, Tianjin, China, in 1998, and is currently working toward the Ph.D. degree in electronics at Carleton University, Ottawa, ON, Canada.

His research interests include neural networks, modeling, and their applications in CAD for electronics circuits.

Mr. Xu was the recipient of the IEEE Microwave Theory and Techniques Society (IEEE MTT-S)

International Microwave Symposium (IMS) Student Paper Award in 2001, the 2002–2003 Ontario Graduate Scholarship in Science and Technology, the 2002–2003 Ontario Graduate Student Scholarship, and the 2003–2004 Ontario Graduate Student Scholarship.



**Qi Jun Zhang** (S'84–M'87–SM'95) received the B.Eng. degree from the East China Engineering Institute, Nanjing, China, in 1982, and the Ph.D. degree in electrical engineering from McMaster University, Hamilton, ON, Canada, in 1987.

He coauthored *Neural Networks for RF and Microwave Design* (Boston, MA: Artech House, 2000), coedited *Modeling and Simulation of High-Speed VLSI Interconnects* (Boston, MA: Kluwer, 1994), and contributed to *Analog Methods for Computer-Aided Analysis and Diagnosis*, (New York: Marcel Dekker, 1988). He was a Guest Co-Editor for the “Special Issue on High-Speed VLSI Interconnects” of the *International Journal of Analog Integrated Circuits and Signal Processing* (Boston, MA: Kluwer, 1994) and was twice a Guest Editor for the “Special Issues on Applications of ANN to RF and Microwave Design” of the *International Journal of RF and Microwave Computer-Aided Engineering* (New York: Wiley, 1999, 2002).

Dr. Zhang is a member of the Professional Engineers Ontario, Canada.